

New observable for gravitational lensing effects during transits

Shinta Kasuya*, Mitsuhiro Honda and Risa Mishima
Department of Information Sciences, Kanagawa University, Kanagawa 259-1293, Japan

Accepted 2010 October 4. Received 2010 October 2; in original form 2010 September 10

ABSTRACT

We investigate gravitational lensing effects of an extrasolar planet transiting its host star. We focus on the ‘rising spikes’ of the light curve just before and after the transit, which is a peculiar feature of the gravitational lensing, and find that it could be a novel observable for determining physical parameters. Detectability of such an effect is also discussed.

Key words: gravitational lensing; micro – eclipses – occultations

1 INTRODUCTION

Observations of decrease of starlight by a transit of an extrasolar planet is one of the important method not only for finding the planet itself but for determining physical parameters of the transiting planet (See e.g. Cassen et al. 2006). Roughly speaking, there are two observables in the transit light curve: Duration and depth. The latter gives the planet radius if the star radius is known, while the former leads to the planet orbital radius if one neglects the size and mass of the planet for the transit duration and the orbital velocity of the planet, respectively.

There is often observations of the orbital velocity and the period of the transit using the Doppler effects in addition to the transit observation (See e.g. Cassen et al. 2006). Hence the planet mass can be determined uniquely, since the inclination is known to be near edge-on from the transit

To date, hundreds of the extrasolar planets are observed by various methods mostly by Doppler method and transits¹, but those with a large orbital radius more than ~ 10 au are limited by these methods. This is because one could see the transit practically only once, at most, in one’s life time, and such planets are also difficult to detect with the Doppler method.

As the distance between the star and the planet becomes larger, the mass of the planet could in principle affect the transit light curve due to microlensing effect. Microlensing with occultation has been considered generally or in other context (Maeder 1973; Bromley 1996; Marsh 2001; Bozza et al. 2002; Agol 2002; Beskin & Tuntsov 2002; Agol 2003; Sahu & Gilliland 2003; Lee et al. 2009). It makes the depression shallower, and steepens the slope of the ingress and egress of the dip (Marsh 2001). However, the former

can be explained by a smaller planet radius, while the latter could be due to a faster transiting velocity.

A peculiarity of the microlensing effect on the transit light curve would be ‘rising spikes’ just before and after the transit.²This is what we focus on in the present article, and we show that the height of the spike has different parameter dependence from other observables such as the depth of the light curve. In particular, it could be measurable in high precision observations such as by *Kepler* or other future facilities.

The structure of the article is as follows. In the next section, we consider both microlensing and occultation simultaneously to obtain the magnification of the starlight. We see typical observables from the transit light curve, and define a novel observable as the ‘rising spike’ in the lensed case in Sec. 3, so that we consider three observables: The depth, the duration, and the rising spike. In Sec.4, we show that the section of isosurfaces of these three observables will determine the physical parameters of the planet: The mass, the radius, and the orbital radius. In Sec. 5, we include the limb darkening as an example effect which may obscure the rising spike. We conclude in Sec. 6. Appendices are devoted to the other sections of the isosurfaces of three observables, and the other cases for lensing and occultation in the aligned situation.

2 MICROLENSING AND OCCULTATION

The lens equation for a point mass is written as

$$\beta(\theta) = \theta - \frac{\theta_E^2}{\theta}, \quad (1)$$

² This feature was mentioned for the case which occultation and microlensing effects are equal in Sahu & Gilliland (2003), and investigated for large source case in Agol (2003).

* E-mail: kasuya@kanagawa-u.ac.jp

¹ See <http://exoplanet.eu/>.

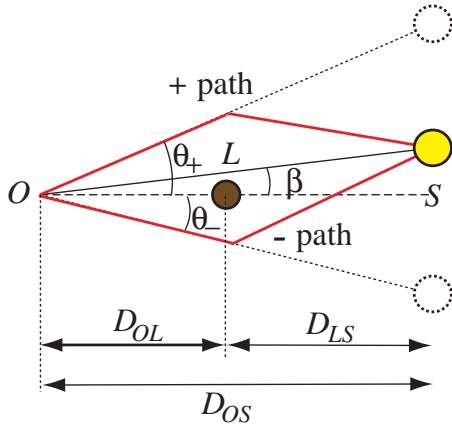


Figure 1. Schematic view of the geometry of the gravitational lensing.

where θ is an angular separation between the lens and the image of the source, while β is that between the lens and the source without lensing (See Fig. 1). θ_E is the Einstein angle,

$$\theta_E = \sqrt{\frac{4GM_L}{c^2} \frac{D_{LS}}{D_{OS}D_{OL}}}, \quad (2)$$

which represents an effective size of the lens. Here D_{OS} and D_{OL} are the distance from the observer to the source and the lens, respectively. D_{LS} is the distance between the lens and the source. M_L is the lens mass, G is the gravitational constant, and c is the speed of light. Solving Eq.(1), we obtain the solutions

$$\theta_{\pm} = \frac{\beta \pm \sqrt{\beta^2 + 4\theta_E^2}}{2}, \quad (3)$$

where $\theta_{+(-)}$ is the angle of the image whose light comes from the far (near) side of the lens, which we will call it $+$ ($-$) path hereafter.

The magnification of the light of a point on the source star through the \pm path is given by

$$A_{\pm} = \frac{d\theta_{\pm}\theta_{\pm}d\phi}{d\beta\beta d\phi} = \frac{1}{2} \pm \frac{\beta^2 + 2\theta_E^2}{2\beta\sqrt{\beta^2 + 4\theta_E^2}}, \quad (4)$$

since the surface brightness is conserved. In the case of microlensing, one cannot discriminate these two magnified images separately, so the observed magnification should be the addition of the two as

$$A(\beta) = A_+ + |A_-| = \frac{\beta^2 + 2\theta_E^2}{\beta\sqrt{\beta^2 + 4\theta_E^2}}. \quad (5)$$

Since the source is usually an extended object, integrating over the source, we can obtain the total magnification as

$$A = \frac{\text{area with lens}}{\text{area without lens}} = \frac{\int A(\beta)\beta d\beta d\phi}{\int \beta d\beta d\phi}. \quad (6)$$

So far we have considered only the point mass lens. Because we are interested in the observation of the transit of a planet in front of the source star, we need to investigate the finite size effect of the lens planet. There are three cases: (1) Both $+$ and $-$ paths of the light from a certain point on the source star are occulted, (2) $-$ path is occulted, or (3) neither path is occulted. Therefore, when integrating over

the source star in the numerator of Eq.(6), we must use $A(\beta)$ itself for case (3), $A_+(\beta)$ for case (2) instead of $A(\beta)$, or do not integrate over the region where case (1) holds.

In the simple configuration that the centres of the lens planet and the source star are aligned, one can calculate the magnification very easily.³ The denominator of Eq.(6) is estimated as

$$\int_0^{2\pi} \int_0^{\theta_S} \beta d\beta d\phi = \pi\theta_S^2, \quad (7)$$

as usual. Here $\theta_S = R_S/D_{OS}$, where R_S is the radius of the source star. In order to calculate the numerator in the transit case when the occultation occurs, we must specify the condition to hold. The occultation takes place if $\beta(\theta_L) > 0$, where $\theta_L = R_L/D_{OL}$ with R_L being the radius of the lens planet (See case I in Fig. A1). It leads to $\theta_L > \theta_E$, which implies that the size of the planet is bigger than that of the lens. Therefore, there is full occultation in the region $\beta < \beta(\theta_L)$, while $-$ path is shielded for $\beta(\theta_L) < \beta < \theta_S$. Thus the numerator of Eq.(6) is obtained as

$$\int_0^{2\pi} \int_{\beta(\theta_L)}^{\theta_S} A_+(\beta)\beta d\beta d\phi = \frac{\pi}{2} \left[\theta_S^2 - \beta_L^2 + \theta_S \sqrt{\theta_S^2 + 4\theta_E^2} - \beta_L \sqrt{\beta_L^2 + 4\theta_E^2} \right], \quad (8)$$

where $\beta_L \equiv \beta(\theta_L)$. Therefore, we have

$$A = \frac{1}{2} \left[1 - \tilde{\beta}_L^2 + \sqrt{1 + 4\tilde{\theta}_E^2} - \tilde{\beta}_L \sqrt{\tilde{\beta}_L^2 + 4\tilde{\theta}_E^2} \right], \quad (9)$$

where the tilde denotes the variable normalised with respect to θ_S such that $\tilde{\beta}_L = \beta_L/\theta_S$ and $\tilde{\theta}_E = \theta_E/\theta_S$. Notice that this magnification (or, more precisely, the diminution) corresponds to the depth at the centre of the transiting light curve. For other situations, see Appendix A.

In order to follow the whole process of the transit, we integrate numerically the numerator of Eq.(6) to estimate the magnification. We show some example of the light curve in Fig. 2. Here we take $M_L = 10M_J$, $R_L = R_J$, and $a = 200$ au, where M_J and R_J are the Jupiter mass and radius, respectively. For parameters of the source star, we set, here and hereafter, $M_S = M_{\odot}$, $R_S = R_{\odot}$, and $D_{OS} = 10$ pc when calculating numerically. We should mention that D_{OS} -dependence is very weak for $D_{OS} \gg D_{LS}$. Also notice that, in this article, we restrict ourselves to the edge-on case in order to focus on the effect of lensing.

3 OBSERVABLES FROM THE LIGHT CURVE AND PHYSICAL PARAMETERS

3.1 Unlensed transit

During the transit a light curve of a star drops down due to the occultation. We can see how much it drops down and how long it lasts. These are the depth and duration of the transit, respectively, and the only observables we can obtain from the light curve (in a simplest case). If we measure the depth at the center of the transit, it is estimated as

³ More general cases can be analytically estimated using elliptic integrals (Agol 2002).

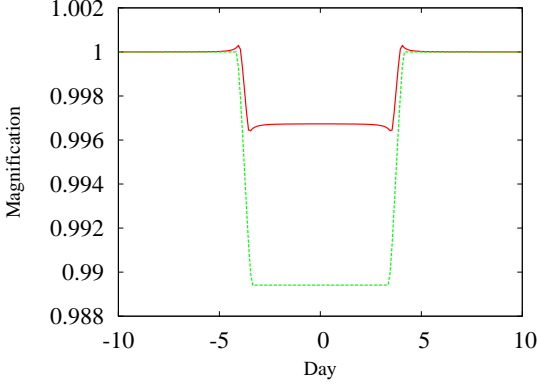


Figure 2. Light curves of the transit. Red (solid) and green (dashed) lines represent the lensed and unlensed cases, respectively. The vertical axis denotes the magnification \mathcal{A} , while the horizontal axis shows the time in day from the centre of the transit in the case of the circular orbit. We take $M_L = 10M_J$, $R_L = R_J$, and $a = 200$ au for the lens planet, and $M_S = M_\odot$, $R_S = R_\odot$, and $D_{OS} = 10$ pc for the source star.

$$\Delta = \frac{\theta_L^2}{\theta_S^2} = \frac{R_L^2 D_{OS}^2}{R_S^2 D_{OL}^2} = \frac{R_L^2}{R_S^2} \left(\frac{D_{OS}}{D_{OS} - a} \right)^2, \quad (10)$$

where $a \equiv D_{LS}$ is the orbital radius of the planet around the star. Once the parameters of the star (R_L and D_{OS}) are known, it could be a function of R_L and a : $\Delta = \Delta(R_L, a)$. On the other hand, the duration of the transit is determined as

$$\begin{aligned} \tau &= \frac{2(\theta_S + \theta_L)}{\omega_L} = \frac{2(\theta_S + \theta_L)}{v_L/D_{OL}} \\ &= 2 \left(R_L + \frac{D_{OS} - a}{D_{OS}} R_S \right) \sqrt{\frac{a}{G(M_S + M_L)}}, \end{aligned} \quad (11)$$

where the planet is assumed to revolve in a circular orbit around the mass center of the star and the planet, and has orbital velocity $v_L = \sqrt{G(M_S + M_L)/a}$. Again, if the parameters of the star (M_L , R_L , and D_{OS}) are known, it becomes a function of M_L , R_L , and a : $\tau = \tau(M_L, R_L, a)$. If M_L could be much smaller than M_S to be neglected, we can derived physical parameters R_L and a from the transit observables Δ and τ . Usually the transit observation is not the only information in our hands. Orbital velocity and/or orbital period of the planet is obtained from the Doppler observation, and three physical parameters are all determined.

3.2 Lensed transit

Neither orbital velocity nor orbital period has been observed by Doppler method if the planet rotates around the star with relatively large orbital radius, typically farther than ~ 10 au. In such a situation, the gravitational lensing effect becomes larger as the lens planet goes away from the star (See Eq.(2)).

The gravitational lensing is known to affect the light curve of the transit in such a way that the depth becomes shallower and the slopes of the ingress and the egress becomes steeper, but the former effect on the light curve can be mimicked by the smaller planet radius, while the latter may imply the faster orbital velocity of the planet. Therefore, one cannot tell if it is really affected by the gravita-

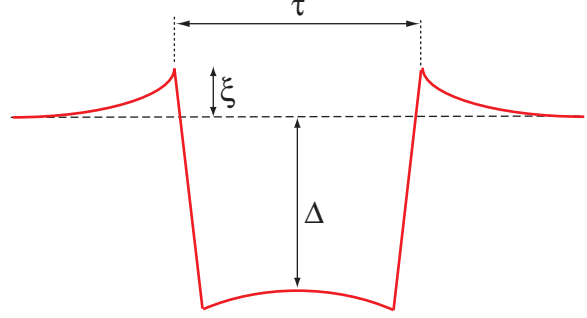


Figure 3. Schematic view of the light curve of the lensed transit.

tional lensing. In order to confirm that one must surely take into account the gravitational lensing effects, their peculiar feature should be observed in the light curve.

Here we claim that the ‘rising spike’ is the smoking gun of the gravitational lensing effect. It is the rise in the light curve just before the ingress (or just after the egress) of the transit, shown as ξ in Fig. 3. There are several key points that the rising spike is a good observable for determining the physical parameters of the planet. First of all, it is a unique consequence of the gravitational lensing effect, and cannot be mimicked by others. The effect could be observed in high precision observation such as the *Kepler*, especially when the orbital radius is relatively large, where the orbital velocity cannot be observed. For parameter determination, it has different parameter dependence from the depth or duration of the transit (Agol 2003). Therefore, it is quite a unique observable.

The amplitude of the rising spike can be calculated from the magnification of the light at the moment when the lensed shadow of the planet has just been tangent to the star as shown in Fig. 4. It is thus given by

$$1 + \xi = \frac{1}{\pi} \int_0^{2\pi} \int_0^1 A_+(\tilde{\beta}(\tilde{\rho}, \psi)) \tilde{\rho} d\tilde{\rho} d\psi, \quad (12)$$

where all the angular separations are normalized with respect to θ_S such as $\tilde{\alpha} = \alpha/\theta_S$, and

$$A_+(\tilde{\beta}) = \frac{1}{2} \left[1 + \frac{\tilde{\beta}^2 + 2\tilde{\theta}_E^2}{\tilde{\beta} \sqrt{\tilde{\beta}^2 + 4\tilde{\theta}_E^2}} \right], \quad (13)$$

with

$$\tilde{\beta} = \sqrt{\tilde{\beta}_x^2 + \tilde{\beta}_y^2}, \quad (14)$$

$$\tilde{\beta}_x = \tilde{\beta}_L + 1 + \tilde{\rho} \cos \psi, \quad (15)$$

$$\tilde{\beta}_y = \tilde{\rho} \sin \psi. \quad (16)$$

Since the image of the source star is not occulted through + path while fully occulted through - path, we can easily calculate ξ using the magnification of the + path for a point mass lens (Witt & Mao 1994; Agol 2002) as

$$\begin{aligned} \xi &= \frac{1}{4\pi \sqrt{(\tilde{\beta}_L + 2)^2 (4\tilde{\theta}_E^2 + \tilde{\beta}_L^2)}} \\ &\quad \times \left\{ (\tilde{\beta}_L + 2)^2 (4\tilde{\theta}_E^2 + \tilde{\beta}_L^2) E(k) \right. \\ &\quad \left. - [\tilde{\beta}_L^2 (\tilde{\beta}_L + 2)^2 + 8\tilde{\theta}_E^2 (\tilde{\beta}_L^2 + 2\tilde{\beta}_L)] K(k) \right. \\ &\quad \left. + 4\tilde{\beta}_L^2 (\tilde{\theta}_E^2 + 1) \Pi(n, k) \right\} - \frac{1}{2}, \end{aligned} \quad (17)$$

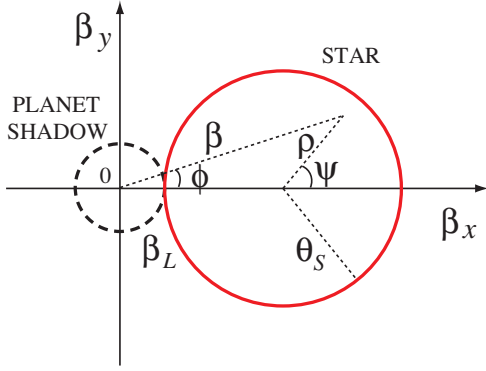


Figure 4. Geometry of the planet and the star at the moment of the peak of the rising spike.

where $K(k)$, $E(k)$, and $\Pi(n, k)$ are the complete elliptical integrals of the first, second, and the third kinds, respectively, and

$$n = 1 - \frac{\tilde{\beta}_L^2}{(\tilde{\beta}_L + 2)^2}, \quad k = \sqrt{\frac{4\tilde{\theta}_E^2 n}{4\tilde{\theta}_E^2 + \tilde{\beta}_L^2}}. \quad (18)$$

Since $\tilde{\theta}_E$ is a function of M_L and a , and $\tilde{\beta}_L$ is a function of R_L , M_L , and a , the rising spike ξ is a function of R_L , M_L , and a : $\xi = \xi(R_L, M_L, a)$.

On the other hand, the depth and duration of the transit are modified due to the gravitational lensing effect. From Eq.(9), the depth is now estimated as

$$\Delta = 1 - \mathcal{A} = \frac{1}{2} \left[1 + \tilde{\beta}_L^2 - \sqrt{1 + 4\tilde{\theta}_E^2 + \tilde{\beta}_L \sqrt{\tilde{\beta}_L^2 + 4\tilde{\theta}_E^2}} \right]. \quad (19)$$

while the duration is given by

$$\tau = \frac{2(1 + \tilde{\beta}_L)}{\tilde{\omega}_L}. \quad (20)$$

Therefore, these two observables are functions of R_L , M_L , and a : $\Delta = \Delta(M_L, R_L, a)$ and $\tau = \tau(M_L, R_L, a)$. Notice that they reduce to the unlensed case (10) and (11), respectively, for vanishing lens mass, $M_L \rightarrow 0$, which implies $\theta_E \rightarrow 0$ and $\beta_L \rightarrow \theta_L$.

4 ISOSURFACES OF THE DEPTH, THE DURATION, AND THE RISING SPIKE

Now we have the depth (19), the duration (20), and the rising spike (17), which depend differently on the three physical parameters of the planet such as the mass M_L , the radius R_L , and the orbital radius a . If these three observables are measured, we can reversely use these equations to determine three physical parameters. Although it could be done in principle, the inverse problem is practically difficult. However, we could numerically obtain the isosurfaces of Δ , τ , and ξ in three dimensions of M_L , R_L , and a . Intersection of these three surfaces must be a point, the solution that we need.

Figure 5 shows sections of the isosurfaces of Δ , τ , and ξ for $M_L = 10M_J$, $3M_J$, and M_J from the top panel to the bottom, respectively. Red, green, and blue lines represent the sections of isosurfaces of the rising spike ξ , the depth Δ , and the duration τ , respectively. Shaded region denotes

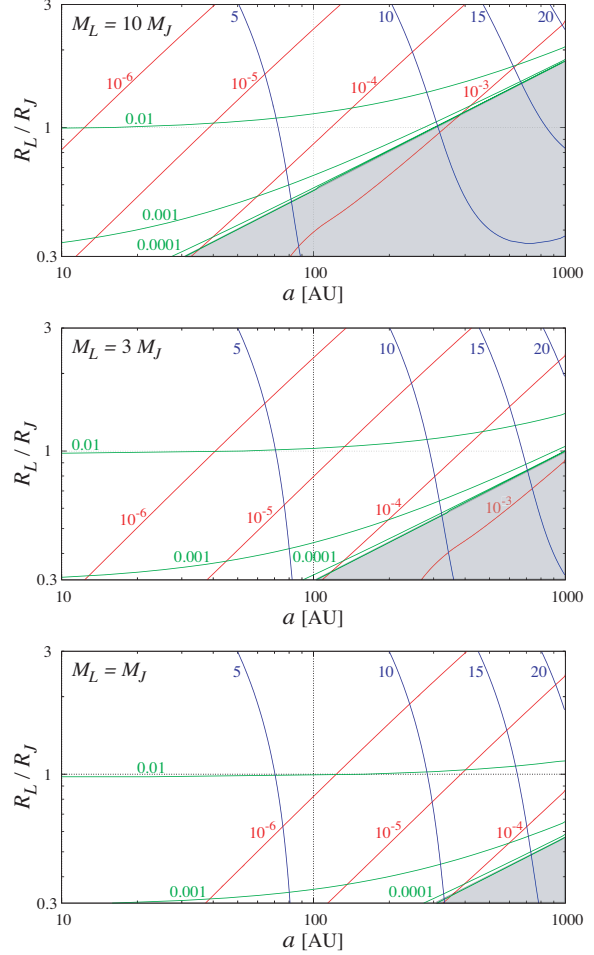


Figure 5. Sections of the isosurfaces of the rising spike ξ (red), the depth Δ (green), and the duration τ in days (blue) for $M_L/M_J = 10, 3$, and 1 , from the top to the bottom panels, respectively. Shaded region represents where the hollow disappears $\Delta < 0$, which we do not consider.

where $\Delta < 0$, which we do not consider because we focus on the transit observation. Since their parameter dependences look quite different in the section with constant M_L , one could derive the physical parameters M_L , R_L , and a from the figure. For other sections, see App. B.

As can be seen in Fig. 5, the rising spike is as large as $\sim 10^{-4}$, which can be measured in high precision observation such as the *Kepler* (Jenkins et al. 2010), for Jupiter-like planets with the orbital radius of a few hundred au. On the other hand, $\xi = 7 \times 10^{-9} - 7 \times 10^{-7}$ for $a = 100 - 1000$ au for those super-earth planets with $M \sim 10M_\oplus$ and $R \sim 3R_\oplus$. Therefore, it has no hope to see the rising spike in these cases.

In order to observe the rising spike, it must last long enough in addition to the height larger than 10^{-4} . Actually, the duration of the transit is about 8 days transit, while the rising spike becomes half the maximum height in 4 hours for $M_L = 10M_J$, $R_L = R_J$, and $a = 200$ au (See Figs. 2 or 6). Therefore, it could well be observed by *Kepler* with the long cadence mode, which has the time resolution of 30 minutes.

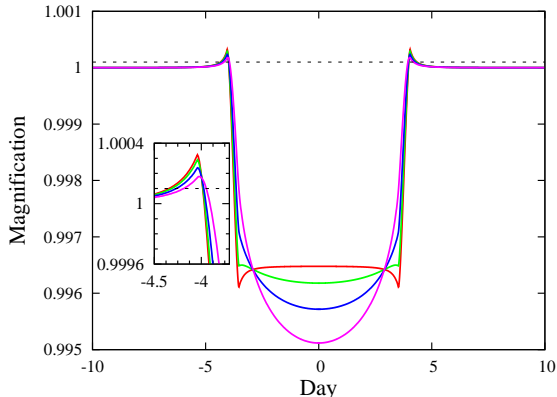


Figure 6. Limb darkened light curves. We take the limb darkening parameters as $(a_1, a_2) = (0, 0)$, $(0.18, 0.10)$, $(0.40, 0.25)$, and $(0.65, 0.35)$, respectively from the top to the bottom at the centre of the transit. Other parameters are set the same as in Fig. 2. In-figure is an enlargement of the rising spikes. Dashed line denotes $\mathcal{A} = 1 + 10^{-4}$.

5 LIMB DARKENING

Realistically, the surface brightness of the source star is not uniform, but has position dependence such that the centre is brighter than the edge. This phenomenon is called the limb darkening of the star. Therefore, one must take this effect into account when any physical consequence is drawn from the light curve of the transit (Agol 2002, 2003). In particular, one may wonder if the rising spike would be round or totally disappear. In this section, we show that this is not the case.

The effect of the limb darkening can be parametrize quadratically as

$$f_{LD}(\cos \mu) = 1 - a_1(1 - \cos \mu) - a_2(1 - \cos \mu)^2, \quad (21)$$

where μ is an angle between the normal of the star surface and the line of the sight, and a_1 and a_2 are constants of $O(0.1)$ (Claret, Diaz-Cordoves & Gimenez 1995). We can calculate the light curve of the transit including limb darkening effects from Eq.(6) with the limb darkening function (21) being inserted into the integrand in both the numerator and the denominator. We show the transit light curve with the typical limb darkening in Fig. 6. Here we plot the case with $(a_1, a_2) = (0.18, 0.10)$, $(0.40, 0.25)$, and $(0.65, 0.35)$ for $M_L = 10M_J$, $R_L = 10R_J$, and $a = 200$ au. One can see that the amplitude of the rising spike would diminish but still be large enough to be observed with the precision of 10^{-4} achieved by *Kepler* (Jenkins et al. 2010) even for a large effect of limb darkening.

A comment is in order. Gravitational lensing effects are also seen as a bump at the bottom of the light curve if the limb darkening is negligible. Although it is another peculiar feature of the lensing, the bump will totally disappear when the limb darkening effect is taken into account, contrary to the rising spike (Agol2003). We thus consider the rising spike as the unique apparent feature of the gravitational lensing effect on the light curve.

6 CONCLUSION

We have studied the gravitational lensing effects on the light curve of the transit which an extrasolar planet plays the role of the lens. The lensing effect becomes sizable only when the orbital radius of the planet becomes larger than ~ 10 au. In such situations, the orbital velocity and/or orbital period are hard to be measured, and it thus seems more difficult to obtain physical informations of the planet. Therefore, it is very important to extract them from the gravitational lensing effects. We have claimed that the rising spike, the sharp rise just before the ingress (or after the egress) of the transit, could be an excellent probe for finding planet parameters. It has a peculiar feature that the height has different dependence on the mass M_L , the radius R_L , and the orbital radius a from other observables, such as the depth and the duration of the transit.

The rising spike can be large enough to be measured in high precision observation such as the *Kepler*, typically when the orbital radius is a few hundred au. It can be observed even if we take into account the limb darkening effect in spite of the fact that other peculiar features of the lensing effect on the transit light curve will be lost.

Since the orbital radius is relatively large, one has at most one chance to observe in one's lifetime. The observability of this kind of the transit could be estimated optimistically as

$$P \sim \frac{t_{\text{obs}}}{T_{\text{orbit}}} \times \frac{R_S}{a} \times N_S \\ \sim \frac{4 \text{ yr}}{3 \times 10^3 \text{ yr}} \times \frac{R_{\odot}}{200 \text{ au}} \times 10^5 \sim 3 \times 10^{-3}, \quad (22)$$

where the first factor is the chance to meet the transit, the second is the probability of the edge-on to the line of the sight, and the last is the number of the stars which will be searched in the *Kepler* in four years of its operation. Although it seems unlikely to find one by *Kepler*, one may observe in the future by using deeper and larger survey.

ACKNOWLEDGMENTS

The work of M.H. is supported by the Grant-in-Aid for Scientific Research from the Ministry of Education, Science, Sports, and Culture of Japan, No. 21740141.

REFERENCES

- Agol E., 2002, ApJ, 579, 430
- Agol E., 2003, ApJ, 594, 449
- Beskin G.M., Tutsov A V., 2002, A&A, 394, 489
- Bozza V., Jetzer Ph., Mancini L., Scarpetta G., 2002, A&A, 382, 6
- Bromley B.C., 1996, ApJ, 467, 537
- Cassen P., Guillot T., Quirrenbach A., 2006, Extrasolar Planets, Springer
- Claret A., Diaz-Cordoves J., Gimenez A., 1995, A&AS, 114, 247
- Jenkins J.M. et al., 2010, ApJ, 713, L120
- Lee C.-H., Riffeser A., Seitz S., Bender R., 2009, ApJ, 695, 200
- Marsh T.R., 2001, MNRAS, 324, 547

Maeder A., 1973, *A&A*, 26, 215Sahu K.C., Gilliland R.L., 2003, *ApJ*, 584, 1042Witt H.J., Mao S., 1994, *ApJ*, 430, 505

APPENDIX A: THREE CASES OF THE MICROLENSING AND THE OCCULTATION

Here we complete the cases of the microlensing and the occultation by the lens planet when the centres of the planet and the star are aligned. The total magnification is given by Eq.(6), and its denominator is obtained as Eq.(7). There are three cases for the microlensing and the occultation: (I) Full, (II) partial, and (III) no occultations, as shown in Fig. A1. Full occultation occurs when $\theta_L > \theta_E$, where both + and - paths are obstructed, while only - path is shielded in the outer region. Therefore, the numerator of Eq.(6) can be written as

$$\begin{aligned} & \int_0^{2\pi} \int_{\beta(\theta_L)}^{\theta_S} A_+(\beta) \beta d\beta d\phi \\ &= \frac{\pi}{2} \left[\theta_S^2 - \beta_L^2 + \theta_S \sqrt{\theta_S^2 + 4\theta_E^2} - \beta_L \sqrt{\beta_L^2 + 4\theta_E^2} \right], \end{aligned} \quad (\text{A1})$$

where $\beta_L \equiv \beta(\theta_L)$. In the case (II), only partial occultation takes place in the outer region, where $\beta(-\theta_L) < \beta < \theta_S$, so that the numerator of Eq.(6) is given by

$$\begin{aligned} & \int_0^{2\pi} \int_0^{\beta(-\theta_L)} A(\beta) \beta d\beta d\phi + \int_0^{2\pi} \int_{\beta(-\theta_L)}^{\theta_S} A_+(\beta) \beta d\beta d\phi \\ &= \frac{\pi}{2} \left[\theta_S^2 - \beta_L^2 + \theta_S \sqrt{\theta_S^2 + 4\theta_E^2} - \beta_L \sqrt{\beta_L^2 + 4\theta_E^2} \right]. \end{aligned} \quad (\text{A2})$$

In the last case, there is no occultation, which is just the same situation as the point mass lens. Thus, the numerator of Eq.(6) becomes

$$\int_0^{2\pi} \int_0^{\theta_S} A(\beta) \beta d\beta d\phi = \pi \theta_S \sqrt{\theta_S^2 + 4\theta_E^2}. \quad (\text{A3})$$

Therefore, the magnification is obtained as

$$\mathcal{A}_{I,II} = \frac{1}{2} \left[1 - \tilde{\beta}_L^2 + \sqrt{1 + 4\tilde{\theta}_E^2} - \tilde{\beta}_L \sqrt{\tilde{\beta}_L^2 + 4\tilde{\theta}_E^2} \right], \quad (\text{A4})$$

$$\mathcal{A}_{III} = \sqrt{1 + 4\tilde{\theta}_E^2}, \quad (\text{A5})$$

where the tilde denotes the variable normalised with respect to θ_S such that $\tilde{\beta}_L = \beta_L/\theta_S$ and $\tilde{\theta}_E = \theta_E/\theta_S$.

APPENDIX B: OTHER SECTIONS OF THE ISOSURFACES OF THE RISING SPIKE, THE DEPTH, AND THE DURATION

The rising spike ξ , the depth Δ , and the duration τ of the transit are functions of three variables: the mass M_L , the radius R_L , and the orbital radius a of the planet. It might be better to draw these isosurfaces in three dimensions, but may be difficult to look at. Therefore, we show some constant M_L sections in Fig. 5, because they seem to have very different curves in those sections. Here we show constant R_L and a sections for completeness in Figs. B1 and B2, respectively. In these figures, two of the observables (ξ and Δ

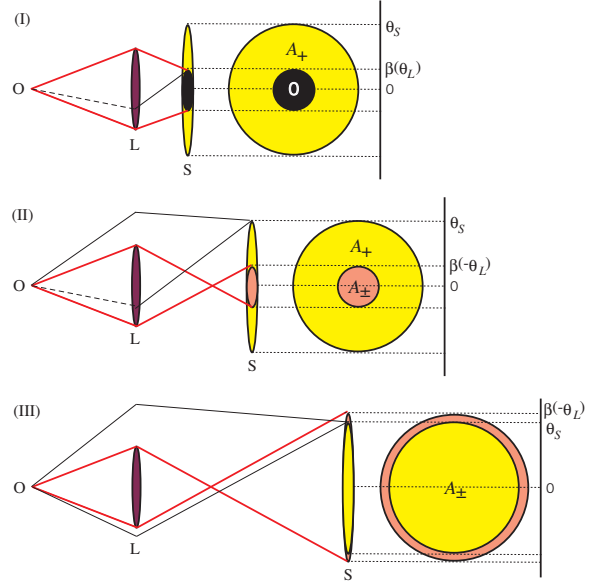


Figure A1. Schematic view of the microlensing and the occultation for three cases: Full, partial, and no occultations from the top to the bottom panels, respectively.

in Fig. B1, while Δ and τ in Fig. B2) have similar dependence on the physical parameters. Notice that one of these parameters (Δ in Fig. B1, while τ in Fig. B2) changes very rapidly with respect to the parameter perpendicular to the two shown in the figures.

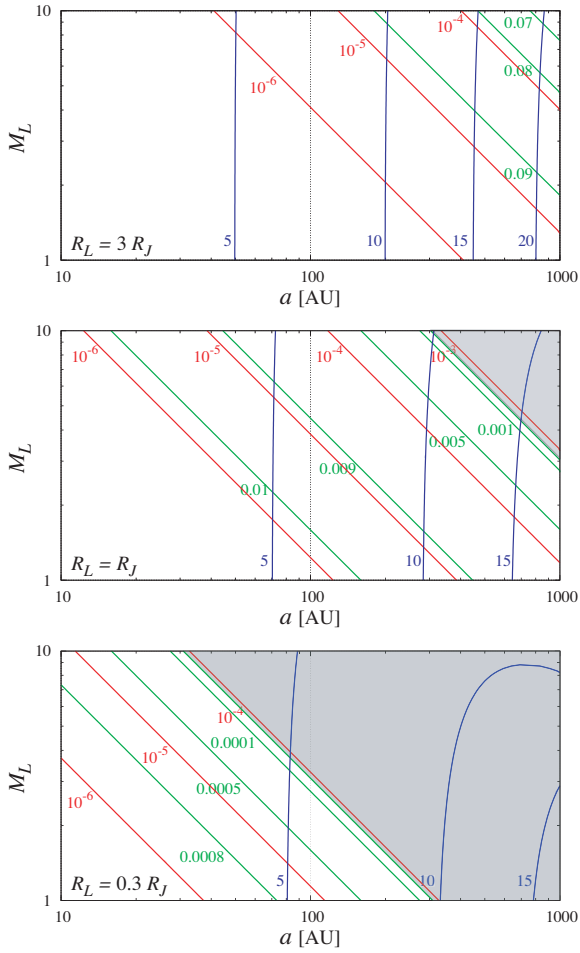


Figure B1. Sections of the isosurfaces of the rising spike ξ (red), the depth Δ (green), and the duration τ in days (blue) for $R_L/R_J = 3, 1,$ and 0.3 , from the top to the bottom panels, respectively. Shaded region represents where the hollow disappears $\Delta < 0$, which we do not consider.

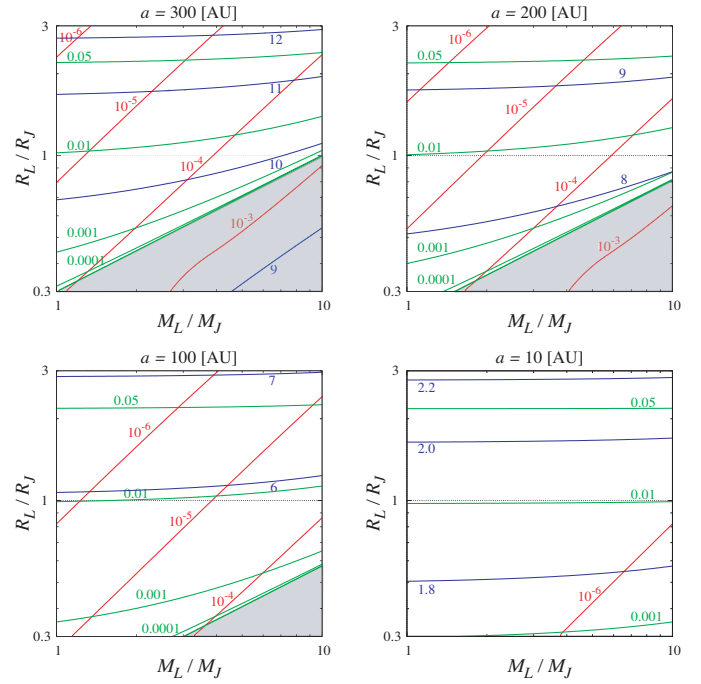


Figure B2. Sections of the isosurfaces of the rising spike ξ (red), the depth Δ (green), and the duration τ in days (blue) for $a = 300, 200, 100,$ and 10 au. Shaded region represents where the hollow disappears $\Delta < 0$, which we do not consider.